Dynamic Friction Models for Longitudinal Road/Tire Interaction: Experimental Results

C. Canudas-de-Wit
Laboratoire d'Automatique de Grenoble
UMR CNRS 5528
ENSIEG-INPG, B.P. 46
38 402 ST. Martin d'Hères, FRANCE
email: canudas@lag.ensieg.inpg.fr

P. Tsiotras and E. Velenis
School of Aerospace Engineering
Georgia Institute of Technology
Atlanta, GA 30332-0150, USA
email: p.tsiotras@ae.gatech.edu

M. Basset and G. Gissinger
Ecole Supérieure des Sciences Appliquées pour l'Ingénieur
Mulhouse, 12, rue des Freres Lumiere
68093 Mulhouse Cedex, FRANCE
email: {m.basset,g.gissinger}@essaim.univ-mulhouse.fr

ABSTRACT
A new dynamic friction force model for the longitudinal road/tire interaction for wheeled ground vehicles is validated via experiments with an actual passenger vehicle. Contrary to common static friction/slip maps, this new dynamic friction model is able to accurately capture the transient behavior of the friction force observed during transitions between braking and acceleration. A velocity-dependent, steady-state expression of the friction force vs. the slip coefficient also allows easy tuning of the model parameters by comparison with steady-state experimental data. Our experimental results validate the accuracy of this new tire friction model in predicting the friction force during transient vehicle motion.

KEY WORDS
Tire Friction, Dynamic Model, LuGre Model, Experiments, ABS

1. Introduction

In the past several years, the problem of modeling and predicting tire friction has become an area of intense research in the automotive community. In particular, ABS and traction control systems rely on knowledge of the friction characteristics. Such systems have enhanced safety and maneuverability to such an extend, that they have become almost mandatory for all passenger vehicles. Therefore, the study of the friction force characteristics at the road/tire interface is of paramount importance for the design of anti-lock brake systems (ABS) and/or traction control systems (TCS). Moreover, tire friction models are also indispensable for accurately reproducing friction forces for simulation purposes. Active control mechanisms, such as TCS, ABS, steering control, active suspension, etc. may be tested and optimized using vehicle mechanical 3D simulators with suitable tire/road friction models.

The most common tire friction models used in the literature are those of algebraic slip/force relationships. They are defined as one-to-one (memoryless) maps between the friction force F, and the longitudinal slip rate s. The most widely used such static model is Pacejka's "Magic Formula" [1]. Other such models have been developed in [2, 3]. These static friction models are appropriate when we have steady-state conditions for the linear and angular velocities of the vehicle. In fact, the experimental data used to validate the friction/slip curves are obtained using specialized equipment that allow independent linear and angular velocity modulation so as to transverse the whole slip range. This steady-state point of view is rarely true in reality, especially when the vehicle goes through continuous successive phases between acceleration and braking. For this reason, kinematic models have been proposed in the literature. A brush model for the longitudinal tire dynamics has been derived in [4, 5].

In this paper, we briefly review the major properties of a new, velocity-dependent, dynamic friction model that can be used to describe the tire/road interaction, developed in [6, 7]. This model has the advantage that it is developed from first principles based on a simple, point-contact dynamic friction model [8]. Hence, the parameters entering the model have a physical significance allowing the designer to tune the model parameters using experimental data. The proposed friction model is also velocity-dependent, a property that agrees with experimental observations. In contrast to other static models, our model is well-defined everywhere (even at zero rotational or linear vehicle velocities) and hence, is appropriate for any vehicle motion situations as well as for control law design. This is especially important during transient phases of the vehicle operation, such as during braking or acceleration.

In order to validate the proposed dynamic friction model for tire/ground interaction, we have collected several actual data using the "BASIL" car which is a laboratory car based on a Renault Mègane 110 Kw. This car is equipped with several sensors in order to study the behavior of the

vehicle during braking and traction phases. We believe that data from an actual passenger vehicle is more relevant than measurements obtained in a highly controlled laboratory environment. We have used the data to first identify the important parameters in our model and then generate the time-histories of the friction forces using our model. The results show excellent agreement between steady-state and transient forces from the experimental results and the simulated friction forces predicted from our model.

2. The LuGre Dynamic Friction Model

A new dynamic friction model (called the LuGre model) for point dry friction has been proposed in [8]. This dry friction model has been extended in [6] in order to capture the complex friction phenomena occurring between the tires and the ground. By introducing a contact patch of length L at the tire/surface interface, we obtain the following partial differential equation for the internal friction state $z(\zeta, t)$ along the patch

$$\frac{\partial z}{\partial \zeta}(\zeta,t)\,|r\omega| + \frac{\partial z}{\partial t}(\zeta,t) = v_r - \frac{\sigma_0|v_r|}{g(v_r)}\,z(\zeta,t) \qquad (1)$$

with $g(v_r) = \mu_c + (\mu_s - \mu_c)e^{-|v_r/v_s|^\alpha}$ where σ_0 is the rubber longitudinal lumped stiffness, σ_1 the rubber longitudinal lumped damping, σ_2 the viscous relative damping, μ_c the normalized Coulomb friction, μ_s the normalized static friction, ($\mu_c \leq \mu_s$), v_s the Stribeck relative velocity, $v_r = r\omega - v$ the relative velocity. The distributed independent variable $z(\zeta, t)$ is the internal friction state that describes the deflection of an elementary rubber element at time t situated at location ζ along the patch. The constant parameter α is used to capture the steady-steady friction/slip characteristic.

The total friction force is given by

$$F(t) = \int_0^L (\sigma_0 z(\zeta,t) + \sigma_1 \frac{\partial z}{\partial t}(\zeta,t) + \sigma_2 v_r) f_n(\zeta) d\zeta \quad (2)$$

where $f_n(\zeta)$ is the normal force density function (force per unit length) along the contact patch.

2.1 Steady-State Behavior

The steady-state characteristics of the model (1)-(2) is obtained by setting $\frac{\partial z}{\partial \zeta}(\zeta, t) \equiv 0$ and by imposing that the velocities v and ω are constant. The resulting expression depends on the normal force distribution $f_n(\zeta)$ along the patch as follows [9]:

- *Constant norm distribution.* For uniform normal load

$$f_n(\zeta) = \frac{F_n}{L}, \quad 0 \leq \zeta \leq L \qquad (3)$$

and one obtains,

$$F_{ss} = \left(\mathrm{sgn}(v_r) g(v_r)\Big[1 - \frac{Z}{L}(1 - e^{-L/Z})\Big] + \sigma_2 v_r\right) F_n \qquad (4)$$

where $Z = |\omega r| g(v_r)/|v_r|\sigma_0$. This simple result has been also reported in [6] and [10].

- *Exponentially decreasing distribution.* In this case, the decrease of the normal load along the patch is approximated with an exponentially decreasing function

$$f_n(\zeta) = e^{-\lambda(\frac{\zeta}{L})} f_{n0}, \qquad 0 \leq \lambda,\ 0 \leq \zeta \leq L \quad (5)$$

where $f_n(0) = f_{n0}$ denotes the distributed normal load at $\zeta = 0$. With the choice (5) one obtains [9]

$$F_{ss} = \sigma_0 c_2 k_1 \Big(1 - e^{-\lambda} + k_2 e^{(-\lambda + c_1 L)} + k_2\Big) + \sigma_2 v_r k_1 (1 - e^{-\lambda}) \qquad (6)$$

where $k_1 = \frac{F_n}{(1-e^{-\lambda})}$, $k_2 = \frac{\lambda}{c_1 L - \lambda}$ and where $c_1 = -\frac{\sigma_0}{g(v_r)}\left|\frac{v_r}{\omega r}\right|$, $c_2 = \mathrm{sgn}(v_r)\frac{g(v_r)}{\sigma_0}$.

Other normal force distributions that satisfy the boundary conditions can also be used; see [7, 9] for details.
Remark: Note that the above expressions can be written in terms of the slip s which is defined by $s = s_b = \frac{r\omega}{v} - 1$ if $v > r\omega$ and $v \neq 0$ (braking) and $s = s_d = 1 - \frac{v}{r\omega}$ if $v < r\omega$ and $\omega \neq 0$ (driving). Comparisons with the steady-state expressions (such as the "Magic Formula") can therefore be made. The expressions (4) and (6) depend not only on the slip s, but also on either the vehicle velocity v or the wheel velocity ω, depending on the case considered (driving or braking). Therefore static plots of F vs. s can only be obtained for a specified (constant) velocity. This dependence of the steady-state force/slip curves on vehicle velocity is evident in experimental data found in the literature. Nonetheless, it should be stressed here that it is impossible to reproduce such a curves form experimental data obtained from standard vehicles during normal driving conditions, since v and ω cannot be independently controlled. For that, specially design equipment is needed. Figure 1(a) shows the steady-state dependence on the vehicle velocity for the braking case, using the data given in Table 1.

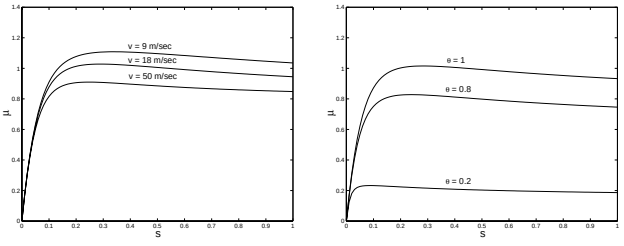

Figure 1. Static view of the distributed LuGre model with uniform force distribution (braking case) under: (left) different values for v, (right) different values for θ with $v = 20\,\mathrm{m/s} = 72\,\mathrm{Km/h}$. These curves show the normalized friction $\mu = F(s)/F_n$, as a function of the slip velocity s.

The level of tire/road adhesion, can be modeled by introducing a multiplicative parameter θ in the function $g(v_r)$ as follows $\tilde{g}(v_r) = \theta g(v_r)$,. Computation of the function $F(s, \theta)$, as a function of θ, gives the curves shown in Fig. 1(b).

Table 1. Data used for the plots in Fig. 1

Parameter	Value	Units
σ_0	181.54	[1/m]
σ_2	0.0018	[s/m]
μ_c	0.8	[-]
μ_s	1.55	[-]
v_s	6.57	[m/s]
L	0.2	[m]

We note that the steady-state representation of equations (4) can be used to identify most of the model parameters by fitting this model to experimental data. These parameters can also be used in a simple one-dimensional lumped model, which can be shown to suitably approximate the (average) solution of the partial differential equation (1). This approximation is discussed next.

3. Average Lumped Model

Although the distributed model (1)-(2) captures reality better than a lumped, point contact model it is desirable to have a discrete/lumped model that is capable of capturing the essential friction characteristics. This can be achieved by defining a *mean friction state* $\bar{z}$ for each tire and then deriving an *ordinary differential equation* for $\bar{z}$. This will simplify the analysis and can also lead to much simpler control design synthesis procedures for tire friction problems. Following [9], if we define the *average friction state* as

$$\bar{z}(t) \equiv \frac{1}{F_n}\int_0^L z(\zeta,t) f_n(\zeta) d\zeta \tag{7}$$

we obtain the following ordinary differential equation

$$\dot{\bar{z}}(t) = v_r - \frac{\sigma_0|v_r|}{g(v_r)}\bar{z}(t) - \kappa(t)|\omega r|\bar{z}(t) \tag{8}$$

$$F(t) = \left(\sigma_0\bar{z}(t) + \sigma_1\dot{\bar{z}}(t) + \sigma_2 v_r\right) F_n \tag{9}$$

where F_n is the total normal force, given by $F_n = \int_0^L f_n(\zeta)\, d\zeta$.

The value of κ in (8) depends on the normal force distribution:

- *Parabolic Distribution.* In the case of parabolic normal force distribution κ takes the values [9, 7] $1/L \leq \kappa \leq 2/L$.
- *Exponentially Decreasing Distribution.* Assuming (5) one obtains $\kappa = \lambda/L$, with $\lambda \geq 0$.
- *Uniform Normal Distribution.* The case of the uniform normal distribution can be viewed as a special case of (5) with $\lambda = 0$. In this case one obtains $\kappa(t) = \kappa_0(t)/L$. The function $\kappa_0(t)$ is chosen in [10] so that the steady state solutions of the total friction force for the average/lumped model in (8)-(9), and the one of the distributed model (4) are the same. This approximation results in the following expression for κ_0

$$\kappa_0 = \kappa_0(Z) = \frac{1 - e^{-L/Z}}{1 - \frac{Z}{L}(1 - e^{-L/Z})} \tag{10}$$

In [10] it is also shown that, such a κ_0 belongs to the range $1 \leq \kappa_0(t) \leq 2$ for all $t \geq 0$. Often, a constant value for $\kappa_0 \in [1, 2]$ can be chosen, without significantly changing the steady states of the distributed and lumped models [9].

4. Experimental Results

In this section we present experimental results used to validate the average dynamic friction model in (8)-(9). We first give the measurements collected during three brakings of a specially equipped test vehicle. The measurements for the three brakings were taken under the same vehicle operational and road conditions. We have used this data to identify the parameters of the average/lumped LuGre tire friction model. We then used these parameters to validate the dynamic friction model by comparing the time histories of the friction force predicted by our model with the friction force from the three experiments.

4.1 Testbed Car Description

The friction data were collected using the "BASIL" car which is a laboratory car based on a Renault Mègane 110 Kw. The car is equipped with several sensors to study the behavior of the vehicle during braking and traction phases. These sensors are (see Fig. 2):

- an optic cross-correlation sensor that measures the transverse and longitudinal vehicle velocities
- a basic inertial unit with a piezoelectric vibrating gyroscope that measures the yaw rate; a separate sensor measures the roll velocity
- a magnetic compass that provide directional information
- two acceleration sensors that measure the longitudinal and lateral accelerations
- an ABS-system used to derive – via suitable signal processing – the wheels' velocities; the ABS system was not enabled during the experiments, it was used only as a wheel velocity sensor
- a Differential GPS system used to locate the vehicle and compute its trajectory with great accuracy (less than one centimeter); this allows repeated experiments at the same road location
- other specific-purpose sensors (not described herein) used to measure the throttle angle (which reflects the command acceleration) and collector pressure (which reflects the braking command)

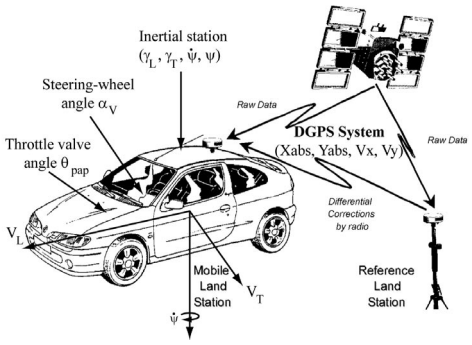

Figure 2. Sensors and measurement parameters.

For this application, a Kistler wheel force transducer has been installed at the place of the standard right rim to measure the dynamic forces and moments acting between the road and the vehicle at the wheel center. Its inertial effects are small and hence have been neglected. The Kistler sensor gives the complete wrench in real time, namely forces the F_x, F_y, F_z and the moment M_z. These variables are shown in Fig. 3. A schematic of the completely equipped "BASIL" vehicle, along with the corresponding measurement parameters is presented in Fig. 2.

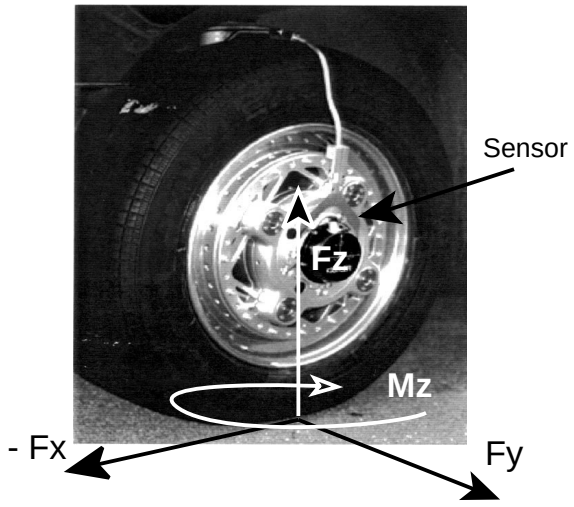

Figure 3. View of the equipped wheel with the Kistler sensor and variables measured.

Experimental procedure: For safety reasons, the trials were carried out on a straight test track under dry weather conditions. After an accelerating phase, the vehicle speed is maintained constant at a pre-defined speed. Then, the test driver releases the clutch for a few seconds in order to match ISO conditions before the braking phase. The ISO conditions are defined as:

- slip velocity near zero value
- steering wheel angle near zero value
- small, approximately constant, values of forces F_x and F_z

The speed of the vehicle decreases slightly down to the desired speed. Then, the test driver starts the braking phase and brakes strongly until the grip limit of the front wheels is reached. Finally, he releases the brake pedal and the front wheels reach again normal grip conditions (small value of slip velocity). Then, the driver accelerates again to repeat the same sequence several times. Three such braking phases were performed and the results were stored in a file for analysis.

4.2 Collected Data

The collected data obtained from the experiments are shown in Figs. 4 and 5. Figure 4 shows the measurements of the braking pressure, the longitudinal speed of the vehicle and the right front wheel (RFW) velocity, for the three braking phases. Figure 5 shows the measurements of the forces F_x, F_y and F_z, and the lateral acceleration G_t. The values of F_y and G_t clearly show the lateral excitation of the vehicle during braking. This is mainly due to geometrical aspects of the suspension system that result in nonzero wheel camber angles.

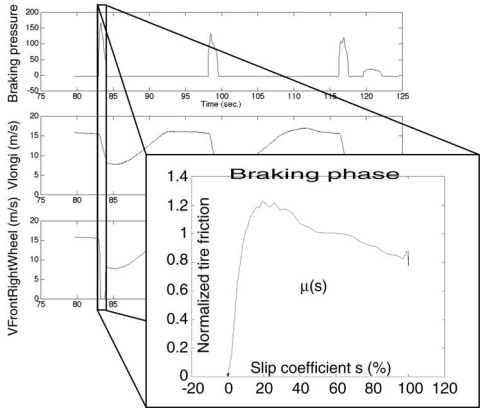

Figure 4. Braking experiments: measurements of the braking pressure, the longitudinal speed of the vehicle and the RFW velocity.

4.3 Parameter Identification

The experimental data consist of measurements of the longitudinal slip s, friction coefficient μ, and linear velocity v. We also know the sampling frequency of the measurements which allows us to re-construct the complete time vector history. The experimental data consist of three distinct brakings shown in Fig. 5. Braking #1 consists of all data collected between 80 and 83.5 sec, Braking #2 consists of all data collected between 97 and 100 sec, and Braking #3 consists of the data collected approximately between 115 and 118 sec; see also the top plot of Fig. 5. First, we

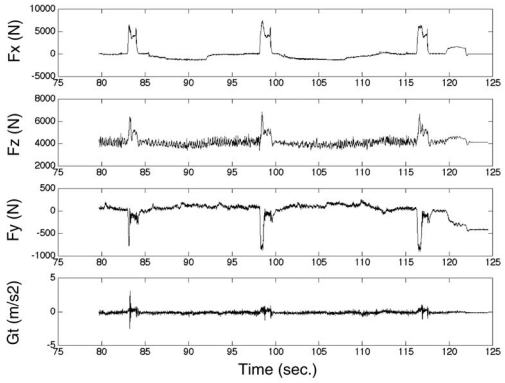

Figure 5. Braking experiments: time-profiles of forces F_x, F_y and F_z, and the lateral acceleration G_t.

compared the 3-D steady-state solution of the distributed dynamical LuGre model at the mean velocity of one of the experiments (Braking #2) with the friction coefficient μ given by the experiments. We then used the $s-\mu$ plot of Braking #2 to identify the parameters for the steady state solution. We plotted the corresponding μ vs. slip curves and determined the parameters of the model ($\sigma_0, \sigma_2, \mu_s, \mu_c$ and v_s). By comparing the time histories of the friction force given by our model, with the ones given by the experiments we can determine the rest of the parameters (e.g., σ_1).

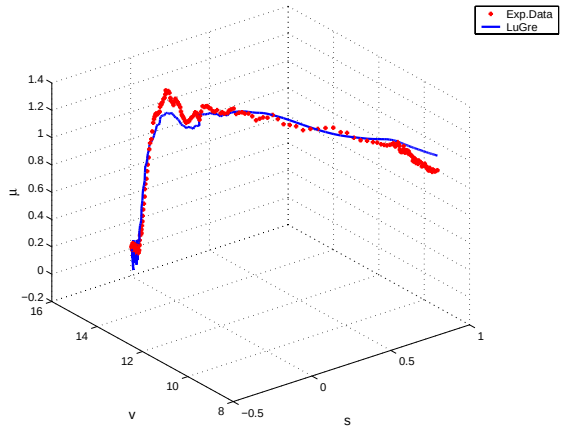

Figure 6. 3-D Plots of the corresponding (μ,s,v) curves for the collected data and the estimated predicted steady-state LuGre average lumped model, with $\alpha = 2$.

In order to identify the model parameters the `lsqnonlin` command of MATLAB was used by fitting the 3-D (μ,s,v) steady-state solution of the distributed model to the data of Braking #2. The command `lsqnonlin` solves an associated nonlinear least squares problem. The previous analysis was done for uniform normal load distribution with $\kappa_0 = 1$ and 2 (case (i)), and with varying κ_0 (case (ii)). The case with exponential normal distribution (5) gives the same results as the ones in Fig. 7 and hence it is omitted. In all cases the patch length was chosen as $L = 0.2\,\mathrm{m}$. The results of the identification algorithm are shown in Table 2.

Table 2. Data used for the plots in Figs 7-8.

Parameter	Value
σ_0	$178\ \mathrm{m}^{-1}$
σ_1	$1\ \mathrm{m}^{-1}$
σ_2	$0\ \mathrm{sec}/\mathrm{m}$
μ_c	0.8
μ_s	1.5
v_s	$5.5\ \mathrm{m}/\mathrm{sec}$

The comparison between the experimental results and the simulation results using the LuGre dynamic friction model for the three cases are shown in Figs. 7-8.

These figures indicate that our proposed model captures very well both steady-state and transient friction force characteristics.

5. Conclusions

Experimental results are presented that corroborate the theoretical developments for a new dynamic tire friction model. This model captures both steady-state and transient effects and is thus more realistic than similar steady-state models. A properly equipped passenger vehicle was used to collect friction measurement data during three successive brakings. These experimental results suggest that the proposed model, although simple, is accurate for analyzing tire friction. It is thus expected that the proposed model will be useful in the automotive community, both for simulation purposes, as well as for control design of ABS and TCS systems.

Acknowledgements: The first two authors would like to acknowledge support from CNRS and NSF(award No. INT-9726621/INT-9996096), for allowing frequent visits between the School of Aerospace Engineering at the Georgia Institute of Technology and the Laboratory of Automatic Control at Grenoble, France. The second author gratefully acknowledges partial support from the US Army Research Office under contract No. DAAD19-00-1-0473.

References

[1] Pacejka, H.B. and Sharp, R.S., Shear Force Developments by Pneumatic Tires in Steady-State Conditions: A Review of Modeling Aspects, *Vehicle Systems Dynamics*, Vol. 20, pp. 121–176, 1991.

[2] Kiencke, U. and Daiss, A., Estimation of Tyre Friction for Enhaced ABS-Systems, In *Proceedings of the AVEG'94*, 1994.

[3] Burckhardt, M., ABS und ASR, Sicherheitsrelevantes, Radschlupf-Regel System, *Lecture Scriptum*, University of Braunschweig, Germany, 1987.

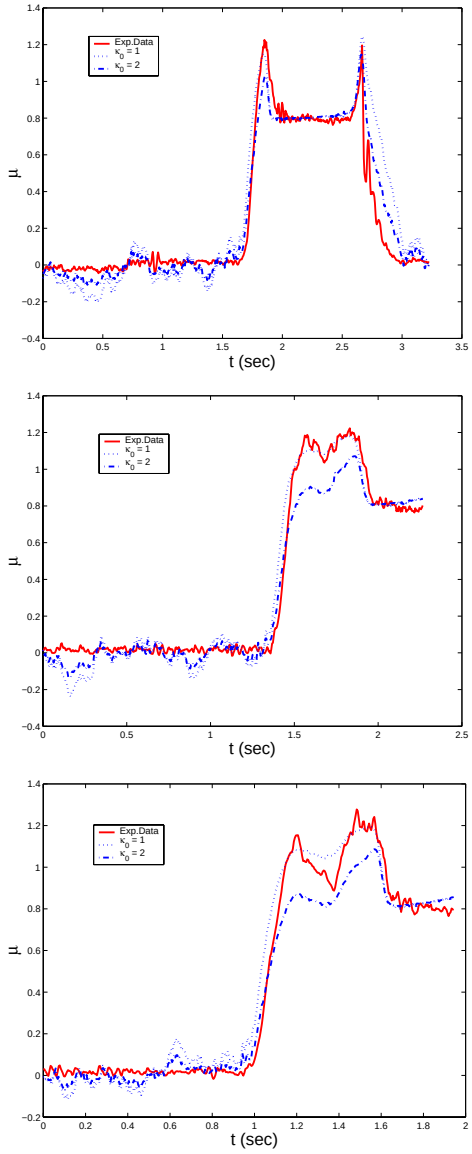

Figure 7. Experimental and simulation results. Case (i): constant $\kappa_0 = 1, 2$. (top) Braking #1, (middle) Braking #2, (bottom) Braking #3.

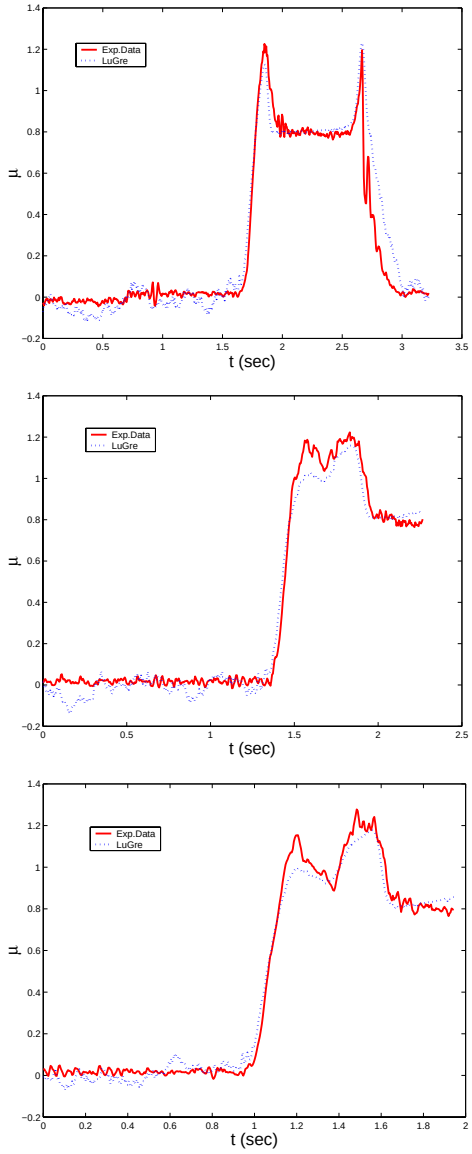

Figure 8. Experimental and simulation results. Case (ii): varying κ_0. (top) Braking #1, (middle) Braking #2, (bottom) Braking #3.

[4] Bernard, J., and Clover, C. L., "Tire Modeling for Low-Speed and High-Speed Calculations," Society of Automotive Engineers, Paper 950311, 1995.

[5] Clover, C.L., and Bernard, J.E., "Longitudinal Tire Dynamics," *Vehicle System Dynamics*, Vol. 29, pp. 231–259, 1998.

[6] Canudas de Wit, C. and Tsiotras, P., "Dynamic Tire Friction Models for Vehicle Traction Control," In *Proceedings of the IEEE Conference on Decision and Control*, Phoenix, AZ, pp. 3746–3751, 1999.

[7] Canudas de Wit, C., Tsiotras, P., Velenis, E., Basset, M. and Gissinger, G., "Dynamic Friction Models for Road/Tire Longitudinal Interaction," submitted to *Vehicle System Dynamics*.

[8] Canudas de Wit, C., Olsson, H., Åström, K.J., and Lischinsky, P., A New Model for Control of Systems with Friction, *IEEE Transactions on Automatic Control*, Vol. 40, No. 3, pp. 419–425, 1995.

[9] Canudas de Wit, C., Tsiotras, P., Velenis, E., Dynamic Friction Models for Longitudinal Road/Tire Interaction: Theoretical Advances, *IASTED Conference on Modelling, Identification and Control (MIC2002)*, Innsbruck, Austria, Feb. 18–21, 2002.

[10] Deur, J., Modeling and Analysis of Longutudinal Tire Dynamics Based on the LuGre Friction Model, In *Proceedings of the IFAC Conference on Advances in Automotive Control*, Kalsruhe, Germany, pp. 101–106 ,2001.